Soils and Foundations 2016;56(1):33–43

HOSTED BY

ELSEVIER

The Japanese Geotechnical Society

Soils and Foundations

www.sciencedirect.com
journal homepage: www.elsevier.com/locate/sandf

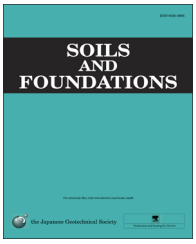

A method to compute the non-linear behaviour of piles under horizontal loading

Gianpiero Russo

Department of Civil, Architectural and Environmental Engineering (D.I.C.E.A), Federico II University, Via Claudio 21, Naples, Italy

Received 24 September 2014; received in revised form 28 July 2015; accepted 16 September 2015
Available online 20 February 2016

Abstract

The empirical evidence for vertical piles under horizontal or lateral loading is firstly reviewed. The load–deflection relationship is nonlinear from the early stages of loading, while the load–moment relationship is nearly linear. Moving from the available experimental evidence, typical design issues are addressed and a validation of the widespread Broms' method is then carried out. To predict the pile–soil interaction, a computer code, NAPHOL, based on a hybrid BEM approach, is fully presented and discussed. A limiting pressure profile, coupled with a cut-off procedure, allows the method to cope with the nonlinear behaviour. Simple guidelines and equations, to calibrate the model parameters, are derived on the basis of the back-analysis of a significant number of case histories. The program is finally used to throw light on the mechanism of the pile–soil interaction under horizontal loading.

Keywords: Analysis; Computer code; Horizontal load; Piles; BEM

1. Introduction

The behaviour of piles under horizontal loading is different from that under vertical loading. When axially loaded, the structural section of the piles does not have a large influence on the pile–soil interaction, as the compression stress is generally very low compared to the strength of the pile material (wood, steel or concrete). With an increasing load, failure may occur, if at all, at the interface between the pile and the soil where the limiting values of the available shaft friction are attained. Under horizontal loading, on the contrary, the piles are primarily subjected to bending moment and shear, and their structural section has a large influence on the pile response both at the serviceability limit state (SLS) and at the ultimate limit state (ULS).

Furthermore, the behaviour of a vertical axially loaded pile depends essentially on the properties of the soil immediately adjacent to the shaft and below the base, which are the zones largely affected by the pile installation process. Accordingly, the behaviour of a vertically loaded pile, particularly its bearing capacity, is markedly affected by the installation process and the technology adopted (Poulos et al., 2001; Mandolini et al., 2005). Under horizontal loading, the pile–soil interaction is confined to a volume of soil which has a different shape and location (Ng et al., 2001; Rollins et al., 2005). Such a volume is typically confined to the upper part of the pile shaft, close to the ground surface, and it develops at a larger distance from the pile shaft. For this reason, a major part of this volume of soil is not affected by the pile installation. However, the available full-scale experimental evidence on piles tested under horizontal loading is less exhaustive than for vertical loading. Furthermore, most of the available horizontal loading tests have been conducted on piles whose heads were free to rotate even though pile heads in actual

E-mail address: pierusso@unina.it
Peer review under responsibility of The Japanese Geotechnical Society.

http://dx.doi.org/10.1016/j.sandf.2016.01.003

foundations are usually fixed. In the next section, some data from horizontal loading tests on piles are firstly reviewed to figure out the main features of the experimental behaviour. The paper proceeds with a short section dedicated to the validation of the widespread Broms' method for the calculation of the ultimate capacity of piles under horizontal loading and to the assessment of the limiting pile–soil interaction pressure. Next, sections are presented in which the computer code, NAPHOL, is described and successfully applied to the back-analysis of well-documented case histories. Some peculiar features of the soil–pile interaction for piles under horizontal loading are highlighted and discussed.

2. Pile behaviour under horizontal loading: experimental evidence

A small number of full-scale horizontal loading tests on piles at the same site, but with different installation techniques, have been reported in the literature. As an example, Fig. 1 shows the results of four loading tests on prefabricated piles carried out in the framework of the Arkansas River Project (Alizadeh and Davisson, 1970).

The subsoil at the site consists mainly of dense sand, and the groundwater table is located very close to the ground level. Piles E7 and F7 were installed by jetting to 8 m and then driving to 15 m; Piles E3 and F3 were driven from the ground surface to the final depth of 15 m. The different installation techniques do not appear to affect the results, while the position of each test pile within the group does seem to have a large influence on the load–displacement curves.

The load–displacement curves obtained by Mori (2003), who tested two different piles in the same sandy gravel subsoil, are compared in Fig. 2. The *Tsubasa* pile is a kind of displacement screw pile; the other pile is an ordinary open-end steel pile driven by vibrations for which the inside soil has been removed. In this case, the installation procedure seems to affect the observed behaviour, namely, the stiffness of the *Tsubasa* pile is higher than that of the open-end steel pile (*Vibration* pile).

According to the above findings and to other available data (Reese and Van Impe, 2001), it can be stated that the influence of the installation technique has sometimes been observed, but that the available data are somewhat contradictory. The influence of both the technology and the installation procedure on the load–displacement curves of the piles under horizontal loading is surely less marked in comparison to the case of piles under vertical loading.

Close scrutiny of the available empirical evidence allows for insight into another feature of the behaviour of piles under horizontal loading.

Ruesta and Townsend (1997), for instance, reported the results of horizontal loading tests on a reinforced concrete prefabricated pile, 16 m in length with a 0.76 m^2 square section, driven into a sandy subsoil (Fig. 3). During the tests, a displacement as high as 15% of the pile width was attained; the test load exceeded the value corresponding to the fissuring of concrete and approached the horizontal bearing capacity, corresponding to the complete yield of the structural section. The pile was instrumented with 8 levels of strain gages which allowed for the accurate determination of the bending moment profile along the shaft at each head load level. These measurements were also supported by a standard inclinometer pipe which was explored by a manual torpedo during the load tests. The load–displacement curve is markedly nonlinear from the very beginning; on the contrary, the load–maximum bending moment curve is nearly linear. Similar results have been obtained by Brown et al. (1987) for tubular piles driven in finely grained soils. In Fig. 4, the load–displacement curve and the head load–maximum bending moment curve are plotted as solid lines together with dashed lines representing the initial tangent of the two curves. This was done to allow for the easy appreciation of the different contributions of nonlinearity to the two experimental curves. In this case, however, the difference between the trends of

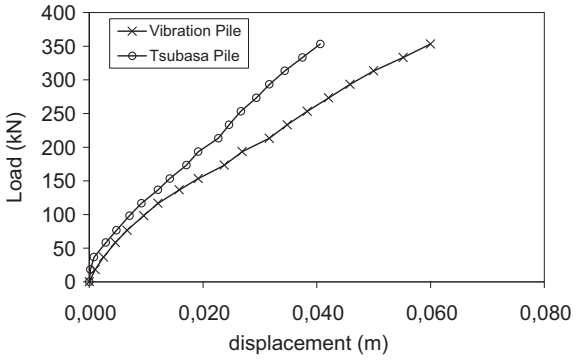

Fig. 2. Horizontal loading tests on displacement screw pile (*Tsubasa*) and an open end tubular vibro-driven pile in the same subsoil (after Mori (2003)).

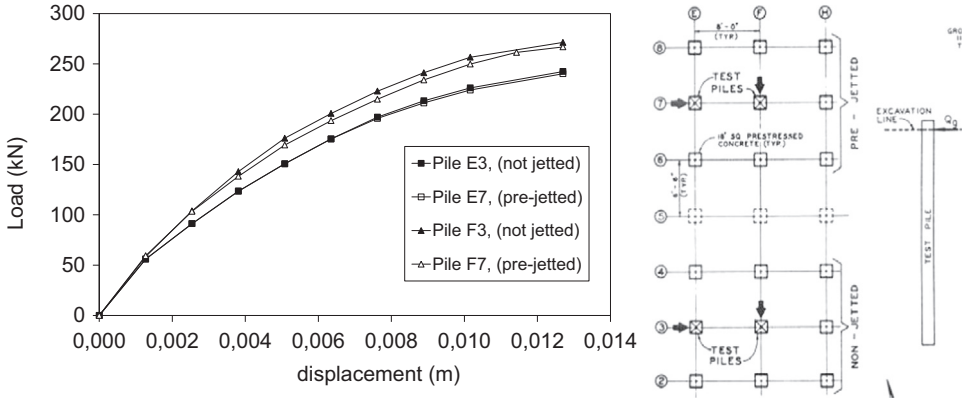

Fig. 1. Horizontal loading tests on four different piles in the same subsoil (after Alizadeh & Davisson, 1970).

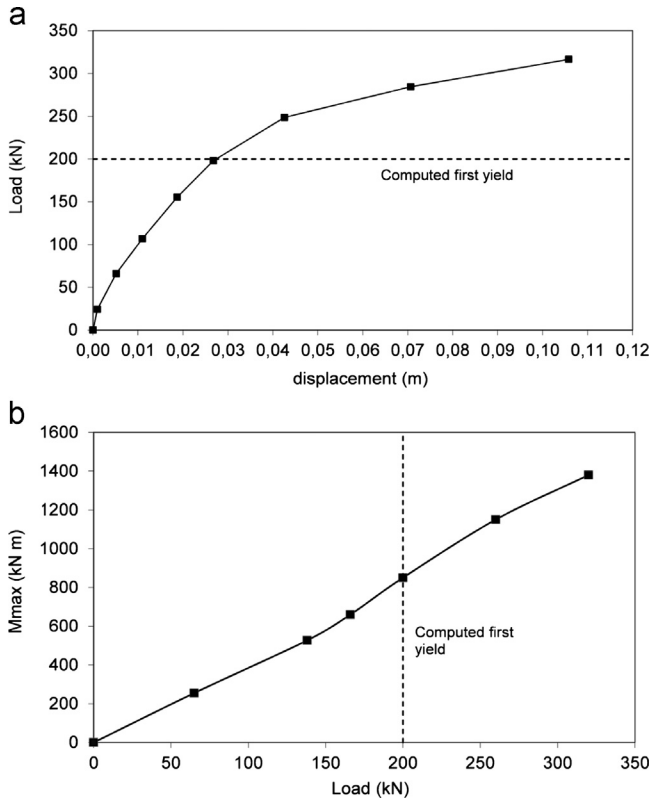

Fig. 3. Load–displacement and load–maximum bending moment relationships (after Ruesta and Townsend (1997)).

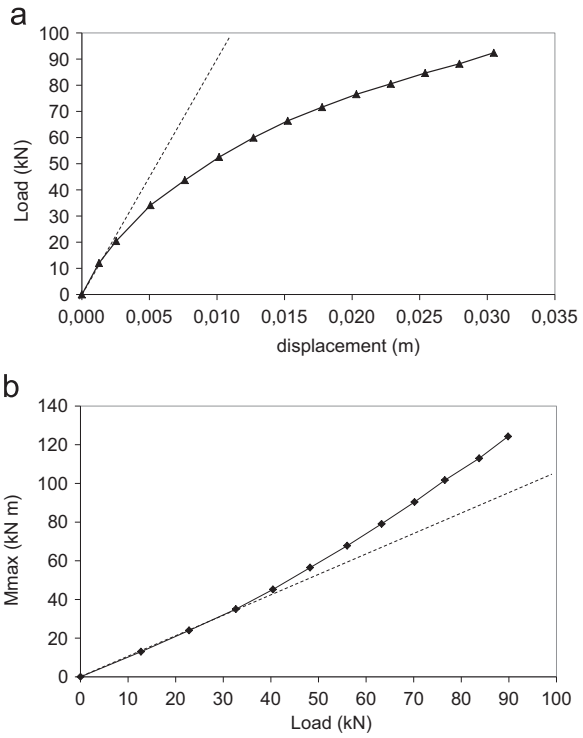

Fig. 4. Load–displacement and load–maximum bending moment relationships (after Brown et al. (1987)).

the two curves is still evident even though it is less significant than that observed for the reinforced concrete pile in Fig. 3. The same trends as mentioned above may be found in quite a number of loading tests available in literature (Mori, 2003; Callisto, 1994; Reese and Welch, 1975).

In this case, the available evidence allows us to state that the lateral load–horizontal displacement relationship of a pile is markedly nonlinear, even at relatively low loading levels; if a reliable prediction of displacement is critical, nonlinearity has to be taken into account. On the contrary, it seems that the maximum bending moment is linked to the applied head lateral load by a nearly linear relationship. This is an interesting observation if the main design issue is a structural one. A tentative explanation could be that the nonlinearity of the soil and that of the pile material combine with each other in determining the load–displacement response. On the contrary, the two sources of nonlinearity may compensate for each other, at least partially, when determining the relative pile-soil stiffness upon which the maximum bending moment along a pile for a given head applied load depends.

3. Analysis and design of single piles under horizontal loading

3.1. Design issues

Traditionally, the first design requirement for any foundation system is to achieve a given safety factor (either globally or partially as a result of the combined application of load multipliers and strength reducers) against bearing capacity failure or the ultimate limit state. The horizontal bearing capacity of a pile, unlike the vertical one, is a function not only of the pile geometry and of the strength of the surrounding soil, but also of the resistance of the structural section of the pile. One of the most widespread methods for evaluating the bearing capacity of piles under horizontal loading is that proposed by Broms (1964a, 1964b). As in many other engineering applications, piles under horizontal loading serviceability limit states must also be checked, even though they are rarely fixed in terms of displacement. In the previous section, the relationship between the horizontal head load and the displacement was shown to be strongly nonlinear due to very low loading levels. However, in many engineering applications, the displacement of a pile under a lateral service load is not a major issue. In some applications, for instance, piles under a retaining wall, the displacement is not only unrestricted, but also encouraged in order to mobilise lower values of the earth pressure behind the wall. On the other hand, most of the existing codes and regulations require that the service bending moments do not exceed a fraction of the flexural resistance of the section. The main aim of this requirement is to prevent the significant opening of cracks and fissures in the concrete. It was already shown that the experimental results often indicate the existence of a simple and almost linear relation between the lateral load and the maximum bending moment along the pile shaft, even at relatively high loading levels. Accordingly, a simple linear model could be adopted for this aim as a design tool.

In the next section, an assessment of Broms' method is firstly reported. In the following paragraphs, the mechanisms of the interaction between the pile and the soil are highlighted and discussed. The discussion focuses on a model for the pile–

soil system implemented into a BEM-based computer code whose capabilities of reproducing the observed behaviour are shown.

3.2. Bearing capacity

The horizontal bearing capacity of a single pile is generally evaluated by the widespread Broms' method, in which the pile and the soil are assumed to behave as rigid–perfectly plastic bodies and the distribution with depth of ultimate lateral pressure p_{ult} on the pile is assumed to depend only on the soil type. The ultimate undrained lateral pressure in clay is assumed as a constant profile in the case of a homogeneous soil layer with the value of $9s_u$, s_u being the undrained shear strength of the clay. The profile is assumed as linearly variable with depth (z) according to the following relationship:

$$p_{ult} = 3K_p \times \gamma \times z \quad (1)$$

In the case of piles embedded in sand, K_p is Rankine's coefficient of passive earth pressure and γ is the unit weight of the soil. These assumptions have been checked by means of a data base (Landi, 2006), including about 40 horizontal loading tests on piles kept very close to failure and sufficiently well documented to allow a back analysis of the results. A comparison between the predicted and the measured horizontal ultimate capacity, H_{lim}, is reported in Fig. 5, separately for clay (a) and for sand (b). In case (a), Broms' method appears to be satisfactory and is reasonably conservative; in case (b), Broms' method tends to underestimate the measured values even by a substantial amount. Similar remarks are made by Kulhawy and Chen (1995) and Fleming et al. (1985), who suggest a slightly different, but improved version, of the Broms' method. The improvement consists simply of the adoption of the ultimate pressure profile suggested for sand by Barton (1984), replacing the profile suggested by Broms (1964a, 1964b) in its original proposal and already mentioned above (Eq. (1)). The ultimate pressure, p_{ult}, proposed by Barton (1984) at depth z, is evaluated with the following equation:

$$p_{ult} = K_p^2 \times \gamma \times z \quad (2)$$

Eqs. (1) and (2) produce very similar results for the friction angles, ϕ, of about 30°, while the higher the values for the friction angle the higher the difference between the two equations, with Eq. (2) by Barton (1984) producing the larger values. In Fig. 6, the comparison between the experimental and the calculated values for the horizontal ultimate capacity, H_{lim}, is repeated only for the case of piles embedded in sand, adopting Barton's pressure profile. The agreement between the experimental and the calculated values is evidently improved as it emerges by the comparison between the diagram in Fig. 6 and the diagram in Fig. 5(b).

3.3. Boundary element method – computer program NAPHOL

The most conventional proposals for estimating the lateral deflection and the bending moments of a laterally loaded single pile or group of piles usually rely on either the theory of subgrade reaction (Matlock and Reese, 1956) or the elastic continuum theory, generally by the Boundary Element Method (Poulos, 1971) or the Finite Element Method (Yang and Jeremic, 2002), or even on hybrid methods (Kitiyodom and Matsumoto, 2002; 2003). The effects of nonlinearity can be taken into account in the theory of subgrade reaction by introducing nonlinear spring characteristics. Such an approach leads to the development of the so-called "p–y" method by Reese et al. (1975). It is also possible to develop nonlinear lateral response solutions from the elastic continuum theory, by imposing the condition whereby lateral soil pressure p cannot exceed an ultimate value p_y (Davies and Budhu, 1986).

A computer program, called NAPHOL (Landi, 2006), based on BEM, has been developed. In this program, the pile is modelled as a linearly elastic beam interacting with a linearly elastic homogeneous and isotropic half space. The pile–soil interface is discretized into n rectangular areas of width d and length $l = L/n$; the distribution of stress acting at the interface is approximated (Fig. 7) by n values of horizontal normal stress p uniformly distributed with constant intensity over each area. The problem is solved by equating the horizontal displacement of the pile to that of the half space, both calculated at the mid-height of each element as a function of the unknown stresses $_{pi}$. Two further equations are obtained by imposing equilibrium between the external forces (horizontal load H and moment M) and the pressure distribution along the pile shaft.

The horizontal displacement at the mid-height of pile element i may be written as

$$y_i = -\sum_{j=1}^{n} \alpha_{ij} Q_j + y_0 + \theta_0 \cdot z_i \quad (3)$$

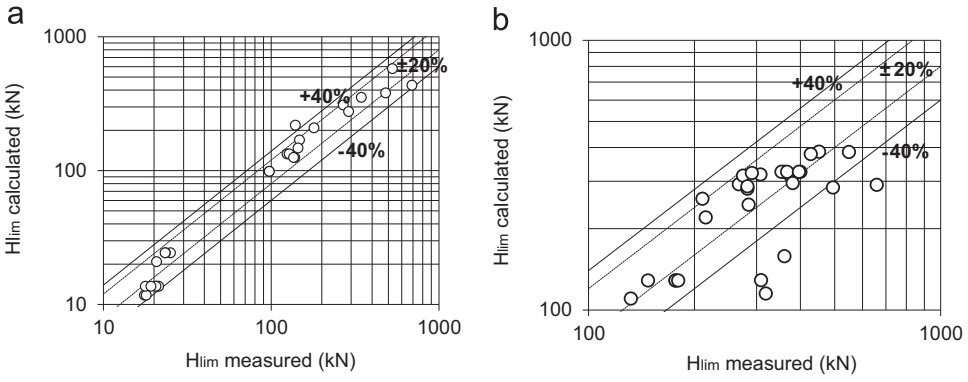

Fig. 5. Calculated (Broms' original method for (a) clay and (b) sand) vs. measured horizontal ultimate capacity Hlim.

with

$$Q_j = p_j dl \tag{4}$$

$$\begin{aligned} \alpha_{ij} &= \frac{z_i^3}{3\,E_pI_p} + \frac{z_i^2(z_j - z_i)}{2\,E_pI_p} \quad \text{if } z_i \le z_j \\ \alpha_{ij} &= \frac{z_j^3}{3\,E_pI_p} + \frac{z_j^2(z_i - z_j)}{2\,E_pI_p} \quad \text{if } z_i > z_j \end{aligned} \tag{5}$$

y_0 and θ_0 represent the unknown horizontal displacement and the rotation at the pile head, respectively, and z_i is the depth of the mid-height of element i-th along the pile shaft. Furthermore, E_p is the Young's modulus of the pile material and I_p is the moment of inertia of the transverse section of the pile. In such a way, the displacement of the points belonging to the pile is expressed as linear functions of the $(n+2)$ unknowns, namely, p_j, y_0 and θ_0.

Horizontal displacement w_{ij}, induced at a point i (corresponding to the mid-height of the i-th element along the pile shaft), belonging to the half space by a horizontal force Q_j applied at point j, can be obtained by the Mindlin (1936) solution, as follows:

$$w_i = \sum_{j=1}^{n} w_{ij} = \sum_{j=1}^{n} b_{ij} Q_j \tag{6}$$

where

$$\begin{aligned} b_{ij} &= \frac{A_{ij} + B_{ij} + C_{ij}}{16\ \pi\ G\,(1-\nu)} \quad G = \frac{E_s}{2\ (1+\nu_s)} \\ A_{ij} &= \frac{(3-4\nu_s)}{R_{1ij}} + \frac{1}{R_{2\ ij}} + \frac{x_{ij}^2}{R_{1\ ij}^3} + \frac{(3-4\nu_s)\,x_{ij}^2}{R_{2\ ij}^3} \\ B_{ij} &= \frac{2\ c_j\ z_i}{R_{2\ ij}^3}\left(1 - \frac{3\ x_{ij}^2}{R_{2\ ij}^2}\right) \quad C_{ij} = \frac{4\,(1-\nu_s)\,(1-2\,\nu_s)}{R_{2\ ij} + z_i + c_j} \\ &\left(1 - \frac{x_{ij}^2}{R_{2\ ij}\,(R_{2\ ij} + c_j + z_i)}\right) \quad r_{ij} = \sqrt{x_{ij}^2 + y_{ij}^2} \\ R_{1\ ij} &= \sqrt{r_{ij}^2 + (z_i - c_j)^2} \quad R_{2\ ij} = \sqrt{r_{ij}^2 + (z_i + c_j)^2} \end{aligned} \tag{7}$$

with E_s, ν_s and G being respectively Young's modulus, the shear modulus and Poisson's ratio of the elastic half space, respectively. The meanings of the geometric symbols are illustrated in Fig. 8.

The unknown soil displacements are again linear functions of the unknown forces Q_j. As stated above, the compatibility is imposed equating the displacement of pile and the soil at the n points:

$$y_i = w_i \qquad i = 1 \text{ to n} \tag{8}$$

The two additional equilibrium equations are written as follows:

$$\sum_{j=1}^{n} Q_j = H \tag{9}$$

$$\sum_{j=1}^{n} Q_j \cdot z_j = -M \tag{10}$$

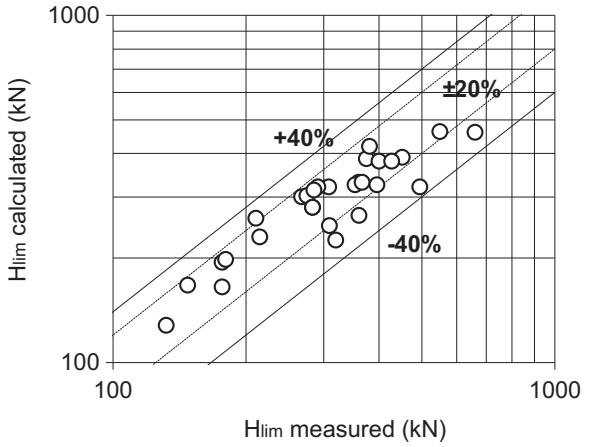

Fig. 6. Calculated (Broms' method adapted with Barton's limiting pressure profile for sand) vs. measured horizontal ultimate capacity Hlim.

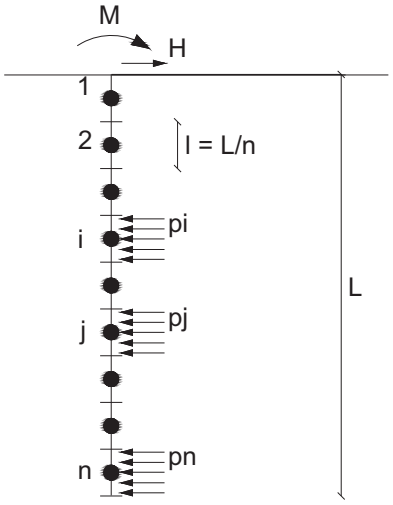

Fig. 7. Pile discretisation and pressure distribution along the pile shaft.

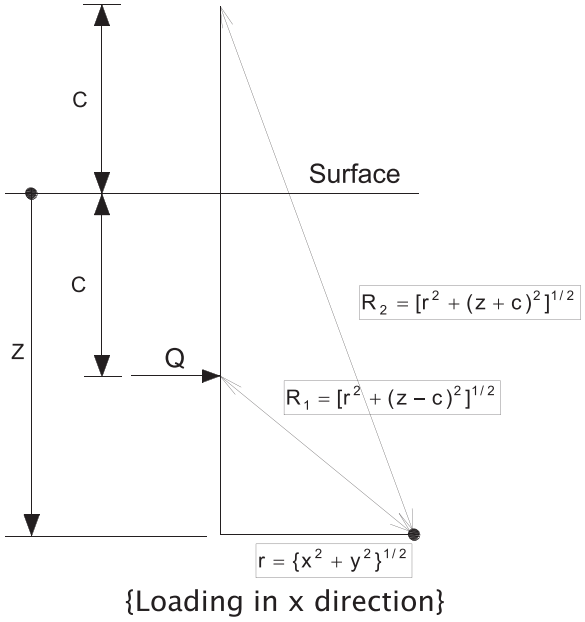

Fig. 8. Geometry of Mindlin's problem and symbols.

The system of $n+2$ linear equations reported above may be solved for the $n+2$ unknowns Q_j, y_0 and θ_0. If the pile head is not free to rotate, the second equilibrium equation is omitted and rotation θ_0 is set to 0. After solving the system, the displacement and the rotation at the pile head may be summarised as

$$y_0 = \frac{H}{E_s L} \cdot I_{yH} + \frac{M}{E_s L^2} \cdot I_{yM} \tag{11}$$

$$\vartheta_0 = \frac{H}{E_s L^2} \cdot I_{\vartheta H} + \frac{M}{E_s L^3} \cdot I_{\vartheta M} \tag{12}$$

If the pile head is not free to rotate, the displacement at the pile head may be expressed as:

$$y_0 = \frac{H}{E_s L} \cdot I_{yF} \tag{13}$$

Poulos and Davis (1980) report exhaustive plots of the various influence factors I as a function of the dimensionless quantities (L/D, υ_s, $K_r = EpI_p/E_sL^4$) in the case of a cylindrical pile embedded in an homogeneous linearly elastic half space.

More generally, the program NAPHOL (Landi, 2006) is capable of solving, even with some approximations, the pile–soil interaction problem for both single piles and pile groups in the following situations:

- horizontally layered elastic soil-when computing displacement w_{ij}, the Mindlin solution is applied by characterizing the layers crossed by the pile shaft by the average of the Young's moduli between points i and j;
- pile with a constant or stepwise variable section;
- nonlinear behaviour of the r.c. pile section (Priestley et al.,1996);
- nonlinear soil behaviour by imposing a limiting pressure at the pile–soil interface.

The limiting pressure in program NAPHOL is an input datum, and different values may be selected for each pile segment corresponding to the different soil layers.

Similar programs exist in the literature as, for instance, the code PRAB (Kitiyodom and Matsumoto, 2002), and most of the options available in NAPHOL are also included in other codes, even though the approximations involved are slightly different. However, the focus of this paper is on laterally loaded single piles and on the calibration of the parameters required for a nonlinear analysis.

3.3.1. Validation and calibration of the program NAPHOL

An extensive validation of the computer code NAPHOL against available experimental evidence has been carried out. The main aim has been to evaluate the capability of the simple elastic–perfectly plastic bilinear model to reproduce the actual nonlinear behaviour of a pile under horizontal loading and to throw some light on the calibrations of the simple model's parameters. The same database adopted for checking Brom's method in Section 3.2 has been explored for applying the code within an exercise of best fitting and changing the value of the input parameters.

In Tables 1 and 2, the main features of the collected case histories are summarised.

Just two examples out of the many back analyses carried out are illustrated and discussed. Reese et al. (1975) reported the results of a horizontal loading test on a driven steel tubular pile with an external diameter of $D=641$ mm, a thickness of $s=12$ mm and a length of $L=15.2$ m embedded in stiff overconsolidated clay. In Fig. 9 the measured load–displacement curve of the pile head is drawn. NAPHOL has been applied by adopting the ultimate pressure profile, as suggested by Broms, for piles in clays and by using s_u values and increasing the depth starting from 25 kPa (at ground level) to 1100 kPa at a depth of 10 m, as suggested by Reese et al. (1975). After several attempts, the undrained Young's modulus was fixed according to the simple relationship $E_u = 800 s_u$, while Poisson's ratio ν_s of the soil was assumed as equal to 0,5 which is usual for undrained analyses of clay. The predicted or calculated load–displacement curve is reported in the same picture showing a remarkable and indeed satisfactory agreement.

Another case history is the one from Brown et al. (1987). They wrote a paper describing the results of an horizontal loading test on a driven steel pipe pile with an external diameter of $D=273$ mm, a thickness of $s=9.3$ mm and a length of $L=13.1$ m embedded in overconsolidated clay. The load–displacement curve is sketched in Fig. 10 (Brown et al. (1987) – after Reese and Van Impe (2001)). NAPHOL has been applied according to the Broms' suggestions for the ultimate pressure profile and using s_u values increasing from 54 kPa (at ground level) to 148 kPa at a depth of 5.5 m, as suggested by Reese and Van Impe (2001). In such a case, the best agreement was found fixing $E_u = 1100 s_u$, while Poisson's ratio ν_s of the soil was assumed as equal to 0.5, which is usual for undrained analyses of clay. The agreement is very satisfactory in this case too.

It should be noted that Reese and Van Impe (2001) used these two case histories to test the computer program LPILE, based on the transfer curve approach. For this reason, the results of the fitting exercise are also reported in Figs. 9 and 10. In Fig. 11, the

Table 1
Main features of the collected case histories for single pile load tests under horizontal load.

Soil type	Number of cases	Field test		Centrifuge test	y_{max}/D (range)
		Steel pipe piles	R.C. piles		
Sand	22	8	9	5	4–12%
Clay	21	13	6	2	3.5–16%

Table 2
Average strength parameters for the case histories analysed in the paper.

	Friction angle, ϕ°		s_u (kPa)	
	Range	Average	Range	Average
Sand	33–45	38-39	–	–
Clay	–	–	20–115	50

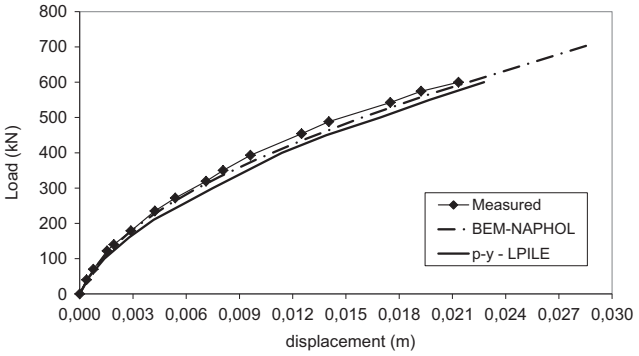

Fig. 9. Comparison between computed and experimental results (after Reese et al., 1975).

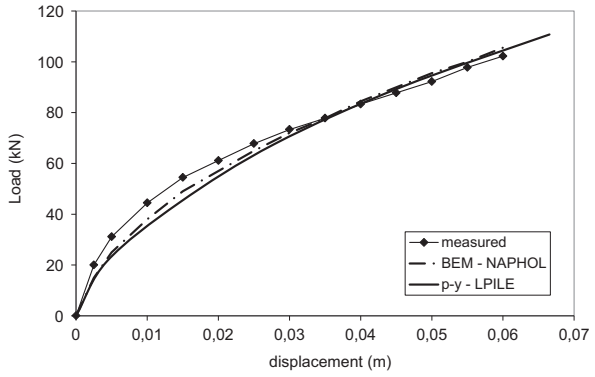

Fig. 10. Comparison between computed and experimental results (after Brown et al. (1987)).

complex shape of the p–y curve that they adopted is sketched; it is considered as typical and needed for OC clays (Reese and Van Impe, 2001). It can be clearly seen, however, that the simple elastic approach with a limiting pressure at the pile–soil interface implemented into the BEM code (push-over analysis) provides the same excellent fit of the observed behaviour as that obtained by the p–y approach based on a rather complex p–y curve. Such a finding, confirmed by the back analyses of quite a number of case histories, definitely shows that the simple bi-linear approach to soil nonlinearity, usually implemented in BEM codes, is by far sufficient for obtaining fairly accurate predictions of the nonlinear load–displacement relationship without the need to adopt more complex p–y functions.

To show the general trend of the agreement obtained between the measurements and the calculations via NAPHOL for all the back-analysed case histories, the plot in Fig. 12 is proposed. The aim of the plot is to show the excellent capability of NAPHOL, with its simple bi-linear approach to soil nonlinearity, to entirely reproduce the measured load–displacement curves for piles pushed either to failure or at least very close to it. For this purpose, the horizontal load, H, measured on the x-axis, is compared to the load calculated via NAPHOL for H calculated at the same displacement level. Each point corresponds to one case history of the database and different markers have been adopted to describe, even briefly, the type of pile and the type of soil. Particularly, the upper plot in Fig. 12a refers to 50% of the maximum test load, while the lower 20% and $\pm$ 50%, are also plotted on the two sides of the segment corresponding to the perfect agreement between calculated and measured loads H, to allow for a simpler and faster evaluation of the quality of the agreement. As shown by both plots in Fig. 12, the agreement is indeed rather satisfactory. When available, even the bending moments measured along the pile shaft were compared with the calculated ones.

The following conclusions are obtained from this best fitting exercise on the basis of a classical trial and error procedure:

i. The best option for piles in clay is to evaluate the limiting soil reaction pressure as $p=9s_uD$ (Broms, 1964a). A slight

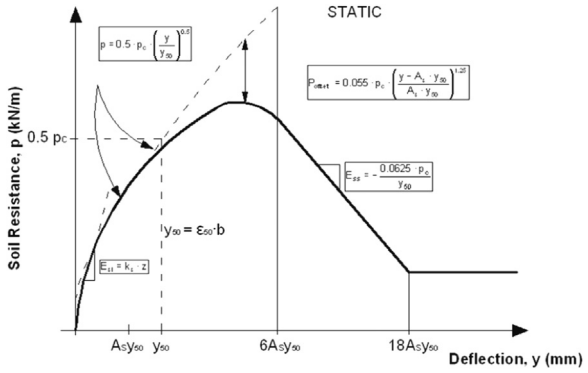

Fig. 11. Suggested p–y curve for piles in stiff OC clay (Reese and Van Impe, 2001).

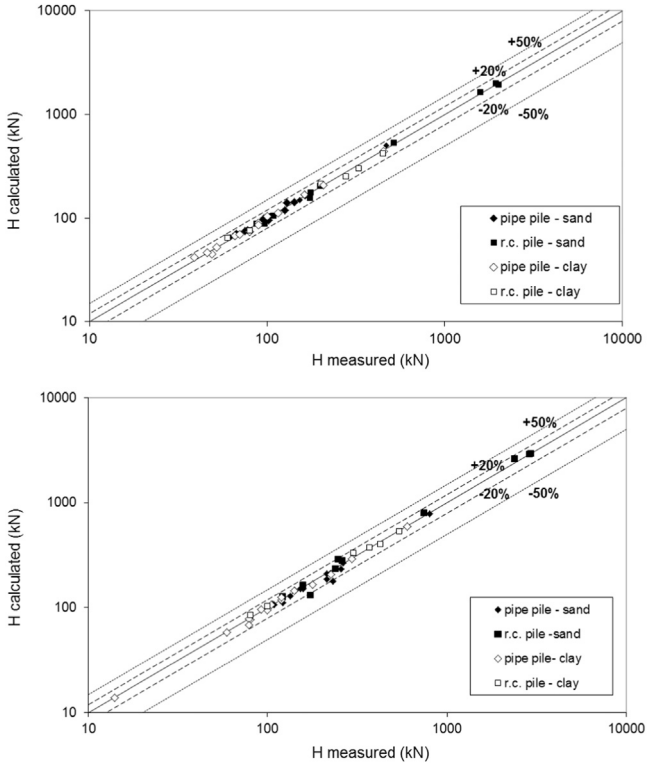

Fig. 12. Comparison between calculated (NAPHOL) and measured head loads, H, for a given pile-head horizontal displacement. (upper plot $y=50\%$ y_{max}–bottom plot $y=95\%$ y_{max}).

improvement is obtained with a new original proposal consisting of the adoption, from the ground level ($z=0$) to the depth $z=D$, of a linear interpolation between $p=0$ and $p=9s_uD$;

ii. The best option for piles in sand is to evaluate the limiting soil reaction pressure according to Eq. (2) (Barton, 1984) which produces a better agreement than Eq. (1). A further improvement is obtained with a new original proposal consisting of the reduction of the limiting soil pressure to the value of $p=K_p\gamma Dz$ applied only near the surface, starting from the ground level ($z=0$) down to the depth $z=D$.

The above modifications proposed to the classical suggestions by Broms (1964a) and Barton (1984) are significant for the agreement between calculated and measured bending moments along the pile shaft. Less important is the influence they have on the load–displacement relationship.

The elastic moduli, which were found as largely influencing the very initial part of the load–displacement relationship, have been fixed according to the following rough suggestions:

for piles in clay $E_u = 700 - 1400\ s_u$ (14)

for piles in sand $E/(\gamma D) = 150\varphi^\circ - 2300$ (15)

More refined approaches to link elastic modulus E to some other quantities, such as plasticity index Ip or overconsolidation ratio OCR, for clay and grain size distributions or the relative density of sand, were substantially unfruitful.

3.3.2. Analysis and mechanisms of pile–soil interaction.

In Fig. 13, a parametric study to show the kind of results produced by the present BEM code, NAPHOL, is reported. An elastic pile ($E_p=28{,}000$ GPa) is subjected to increasing lateral load, while it is embedded in a homogenous elastic half space (E_s, ν_s) adopting the Broms' suggestion for imposing a limiting pressure profile. The parametric study addressed the problem of simulating the case of a pile with a slenderness ratio of L/D=20, embedded in a clay layer with $E_s=E_u=ks_u$, where k is in the range 10–500, $\nu_s=0.5$ and a limit pressure profile defined as $9s_u$ according to Broms (1964a). Having kept undrained shear strength s_u constant in all the analysed cases, both the ratio E_u/s_u and the relative pile–soil stiffness E_p/E_u are variable in the three cases of the parametric study.

The load–deflection curve obtained by NAPHOL is markedly nonlinear, while the load–maximum moment curve is only slightly curved with the concavity upwards. The adoption of a more realistic nonlinear model for the pile material would of course increase the nonlinearity of the load–displacement relationship, while further attenuating the already slight curvature of the load–maximum moment relationship.

It may also be seen that the load–deflection curve is strongly affected by the deformation characteristic of the soil (values of E_s/s_u), while the lateral load–maximum moment relationship is relatively linear and practically unaffected by the relative stiffness of the pile–soil system E_p/E_s. This last conclusion may be somewhat confusing and seem contradictory to what is generally

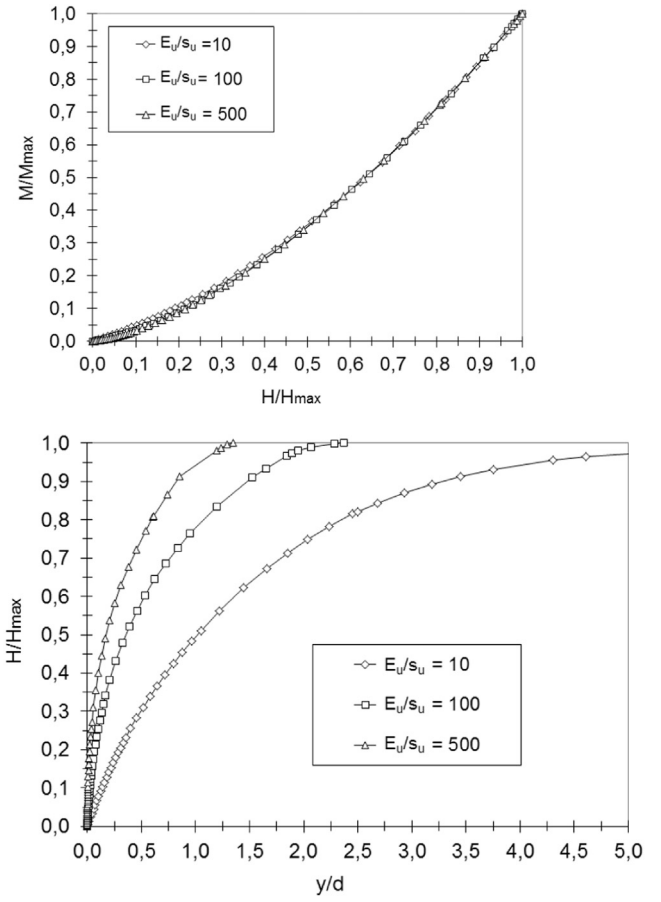

Fig. 13. Sensitivity analysis with BEM code NAPHOL for an elastic pile embedded in clay.

expected, namely, that the interaction between the pile and the soil generating the bending moments along the shaft is affected by the relative soil–pile elastic stiffness.

The reason for these apparently unexpected results is clarified by Fig. 14. In this figure, both the dimensionless profile of the bending moment M(z) and of the pressure profile p(z) with the depth are reported for three load levels ($H/H_{lim}=0.3$–0.5–0.65) and refer to the case of $E_s/s_u=100$. The data are plotted in dimensionless form normalising both the bending moment and the pressure with respect to the maximum calculated value. As is clearly shown, for any value of the applied head load, the mobilised pressure at the pile–soil interface attains its limit value down to about the same depth where the maximum moment occurs. A sort of progressive downward failure mechanism is mobilised at the pile soil interface. This mechanism, and hence, the value of the maximum bending moment, is not significantly affected by the relative elastic stiffness of the pile–soil system, while it is mainly influenced by the limiting pressure profile.

Direct experimental evidence of the above mechanism cannot be easily provided, because there is a substantial lack of measurements of the lateral pressure exerted by the soil on the pile. Some indications, however, may be obtained by double derivations of the measured bending moments profiles. This process is not straightforward and the results are strongly influenced by the details of smoothing and integration. Landi

(2006) proposed a procedure based on cubic *s–p* lines with a preliminary double smoothing procedure.

For the sake of brevity, only the results from two selected case histories of piles in clay (Brown et al., 1987; Ilyas et al., 2004) and two in sand (Remaud et al., 1998; Barton, 1984) are presented in Figs. 15 and 16.

For each case, the profile of the measured bending moments along the pile shaft is reported on the left side, while the

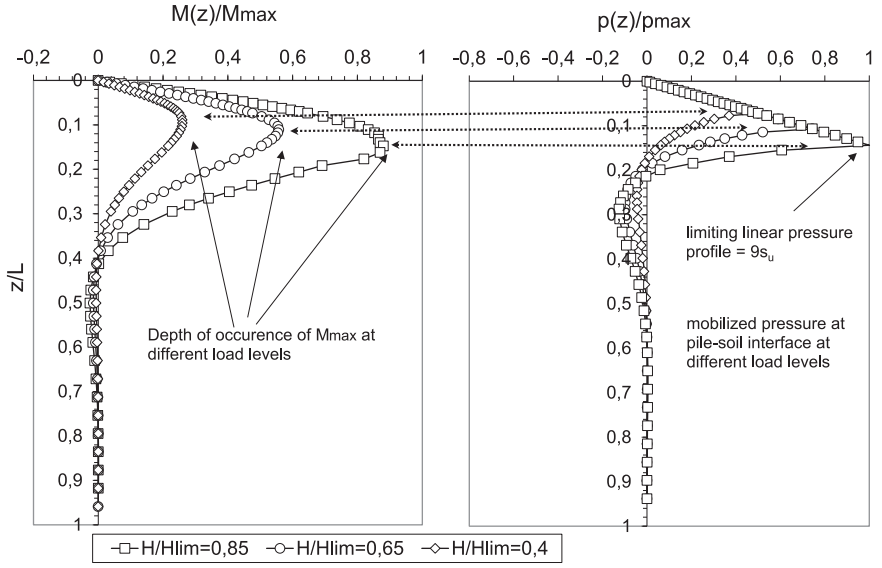

Fig. 14. BEM (NAPHOL) results for an elastic pile embedded in clay (case $E_u/s_u=100$): normalised bending moment $M(z)$ and lateral soil pressure $p(z)$ versus depth, z/L.

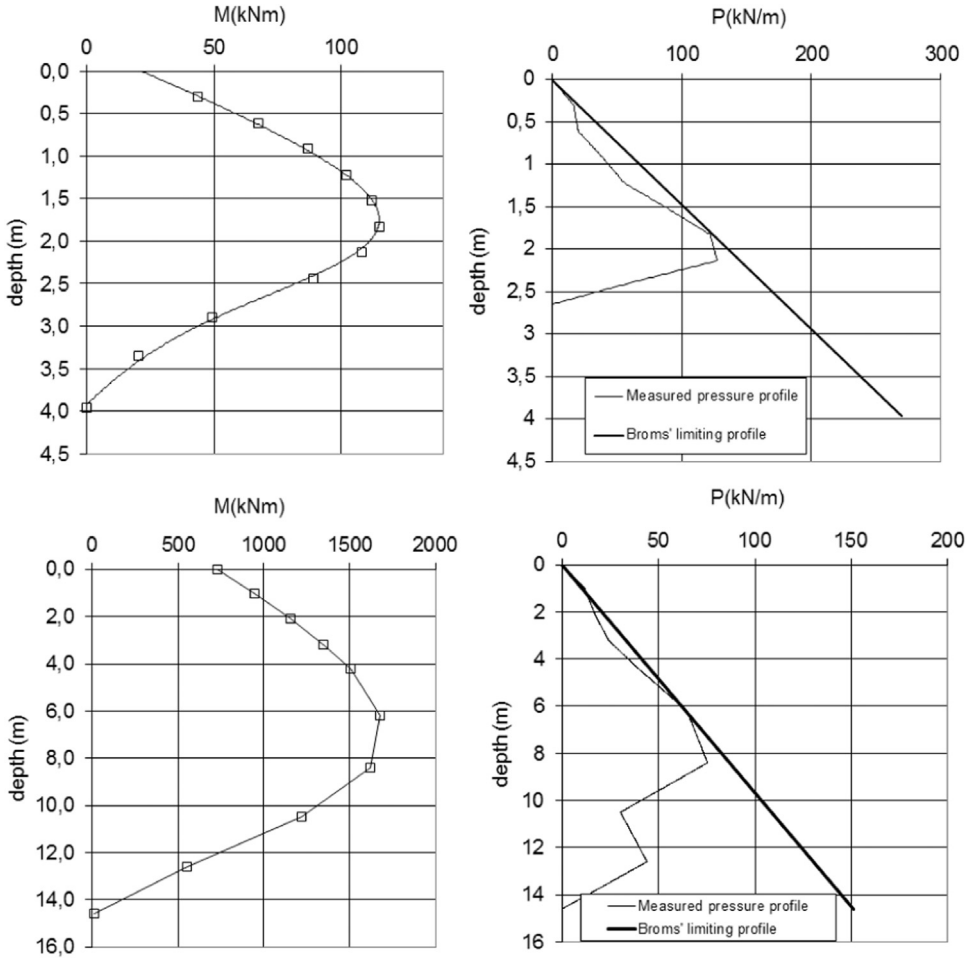

Fig. 15. Measured bending moment and mobilised pressure profile for piles in clay vs. Broms' limiting pressure profile.

corresponding measured pressure profile is compared with the theoretical limiting pressure profiles on the right side. The quantity P(kN/m) reported on the *x*-axis is simply the pressure at the depth z times the diameter of the pile. The limiting profiles adopted here are those suggested by authors like Broms (1964a, 1964b) and Barton (1984) for piles in clay and in sand. These profiles have already been presented and discussed in Section 3.2. Even with some approximation, the experimental data substantially confirm the mechanism clearly revealed by the BEM nonlinear analysis via NAPHOL. In other words, it can be appreciated from the plots on the right side of Figs. 15 and 16 that the full mobilisation of the pressure exerted from the soil onto the pile occurs approximately down to the same depth where the maximum bending moment along the pile shaft is attained.

In the cases of piles in sand, the comparison between Broms' and Barton's profiles (see Eqs. (1) and (2)) shows again the superiority of the latter in providing a more satisfactory agreement with the measured limiting pressures. As already mentioned, the highlighted mechanism may well be mainly responsible for the fact that the bending moment along the pile shaft, even at low load levels, seems more affected by the limiting pressure profile than by the relative elastic stiffness of the pile-soil system typically represented by the simple ratio between the two elastic Young's moduli.

4. Concluding remarks

The available experimental evidence shows that the influence of the installation procedure on the behaviour of piles under lateral loading is less significant than the influence exerted on piles under axial loading. From the same experimental evidence, it is indeed very clear that the load–deflection relationship is markedly non-linear from the early stages of loading. On the other hand the relationship between the applied head load and the observed maximum bending moments is approximately linear up to a very large displacement and even close to failure. It has to be underlined that very often the lateral loading tests are conducted on piles whose heads are free to rotate, while the heads of piles of most actual foundations are fixed.

The main design issues for piles under horizontal loading have been faced and a positive assessment of the widespread Broms' (1964a, 1964b) method for the computation of the ultimate load capacity has been successfully carried out. Various limiting

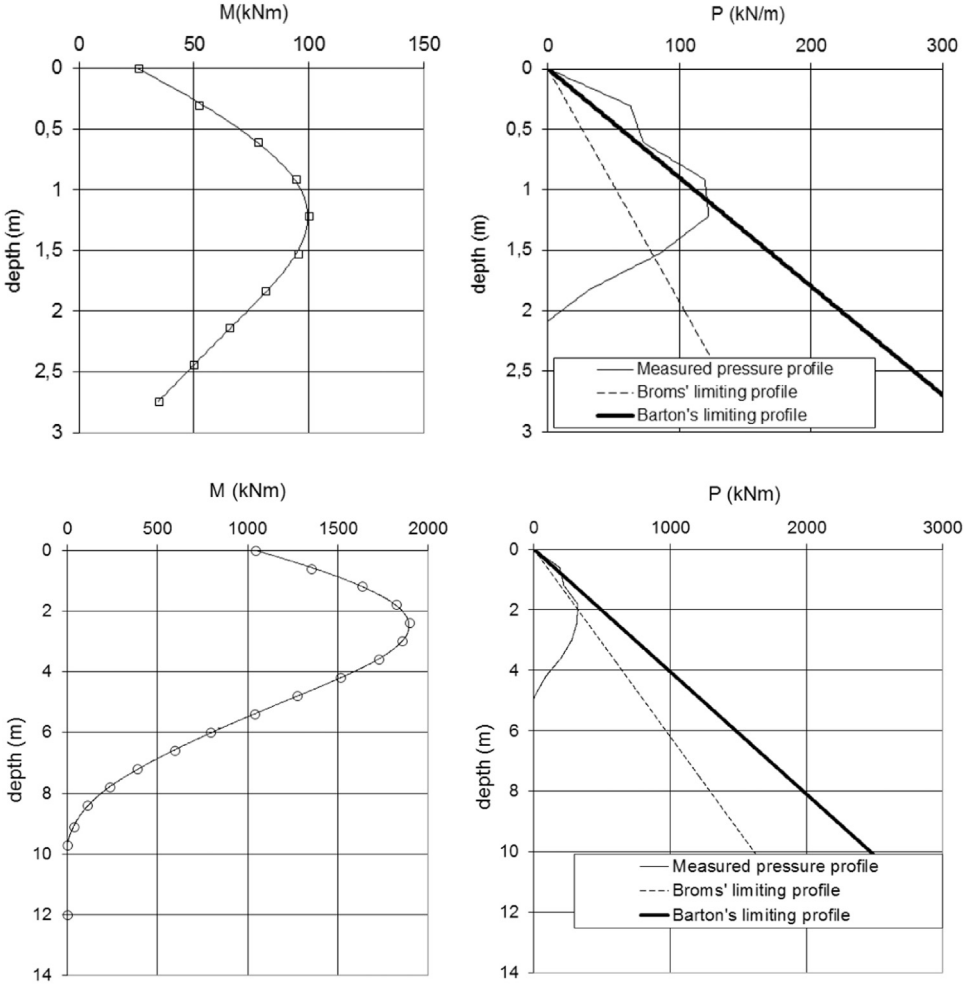

Fig. 16. Measured bending moment and mobilised pressure profile for piles in sand vs. Broms' and Barton's limiting pressure profile.

pressure profiles have been compared to the one suggested by Barton (1984), being the more accurate one for piles in sand.

Subsequently, the issue concerning the load–displacement relationship has been addressed together with an evaluation of the maximum bending moment along the pile shaft. A BEM code, NAPHOL, implementing a relatively simple model of pile–soil interaction, has been described. The nonlinearity of the model derived from the simple imposition of a limiting value for the pile–soil interaction pressure has been calculated on the basis of linearly elastic solutions. A comparison with the experimental results and with the results computed via a more complex p–y curve approach has shown the adequacy of the code and of the simple model in satisfactorily predicting (class c prediction) observed behaviours. Simple equations have been provided to calibrate the parameters of the model for piles in clay or in sand.

The computer code NAPHOL has also been used to throw light on the mechanisms of the interaction between piles and soil. The frequently observed linear relationship between the applied head load and the maximum bending moment along the pile shaft, together with the scarce influence of the relative elastic stiffness, Ep/Es, on this last item, have been substantially explained showing that a sort of progressive downwards failure occurs during the increase in horizontal head load. This mechanism has first been shown to be predicted by NAPHOL, and subsequently, verified on the basis of measurements taken during pile loading tests.

References

Alizadeh, M., Davisson, M.T., 1970. Lateral load tests on piles – Arkansas River Project. J. Soil Mech. Found. Div. 96, 1583–1604.

Barton, Y.O., 1984. Response of pile groups to lateral loading in the centrifuge. In: Proceedings of Symposium on Appl. of Centrifuge Modelling to Geotech. Design, Balkema, Rotterdam, The Netherlands.

Broms, B.B., 1964a. Lateral resistance of piles in cohesive soils. J. Soil Mech. Found. Div. 90, 27–63.

Broms, B.B., 1964b. Lateral resistance of piles in cohesionless soils. J. Soil Mech. Found. Div. 90, 123–156.

Brown, D.A., Reese, L.C., O'Neill, M.W., 1987. Cyclic lateral loading of a large scale pile group. J. Geotech. Eng. 113, 1326–1343.

Callisto, L., 1994. Experimental observations on two laterally loaded bored piles in clay. In: Pile foundations – Experimental investigations, analysis and design, a workshop in Napoli, pp. 349–359.

Davies, T.G., Budhu, M., 1986. Non-linear analysis of laterally loaded piles in heavily overconsolidated clays. Géotechnique 36 (4), 527–538.

Fleming, W.G.K., Weltman, A.J., Randolph, M.F., Elson, W.K., 1985. Piling Engineering. Surrey University Press, Glasgow, 380.

Ilyas, T., Leung, C.F., Chow, Y.K., Budi, S.S., 2004. Centrifuge model study of laterally loaded pile groups in clay. J. Geotech. Geoenviron. Eng. 130 (3), 274–283.

Kitiyodom, P., Matsumoto, T., 2002. A simplified analysis method for piled raft and pile group foundations with batter piles. Int. J. Numer. Anal. Methods Geomech. 26, 1349–1369.

Kitiyodom, P., Matsumoto, T., 2003. A simplified analysis method for piled raft foundations in non homogeneous soil. Int. J. Numer. Anal. Methods Geomech. 27, 85–109.

Kulhawy, F.H., Chen, Y.J., 1995. A thirty year perspective of Broms' lateral loading models, as applied to drilled shafts. Bengt B. Broms Symposium on Geotechnical Engineering, Geotechnical Research Centre, Singapore pp. 225–240.

Landi G, 2006. Piles Under Horizontal Load: Experimental Investigations and Analysis (in Italian). University of Napoli.

Mandolini, A., Russo, G., Viggiani, C., 2005. Pile foundations: experimental investigations, analysis and design, State of the Art Report. In: Proceedings of the XVI International Conference on Soil Mechanics and Geotechnical Engineering, Osaka, Japan, vol. 1, pp. 177–213.

Matlock, M.M., Reese, L.C., 1956. Non dimensional solutions for laterally loaded piles with soil modulus assumed proportional to depth. In: Proceedings of the VIII Texas Conference on SMFE, Special Publ. 29 Univ. Texas, Austin.

Mindlin, R.D., 1936. Force at a point in the interior of a semi-infinite solid. Physics 7, 195–202.

Mori, G., 2003. Development of the screw steel pipe pile with toe wing "Tsubasa Pile". In: Proceedings of the 4th International Geotechnical Seminar on Deep Foundations on Bored and Auger Piles, Ghent, Belgium, June 2003. W.F. Van Impe, 2003 Millpress Rotterdam.

Ng, C.W.W., Zhang, L.M., Dora, C.N.N, 2001. Response of laterally loaded large-diameter bored pile groups. J. Geotech. Geoenviron. Eng. ASCE. 127 (16 No. 8), 658–669.

Poulos, H.G., 1971. Behavior of laterally loaded piles: I – single piles. J. Soil Mech. Found. Div. 97 (5), 711–731.

Poulos, H.G., Davis, E.H., 1980. Pile Foundations Analysis and Design. John Wiley & Sons, 397.

Poulos, H.G., Carter, J.P., Small, J.C., 2001. Foundations and retaining structures – Research and practice. In: Proceedings of the XV International Conference on Soil Mechanics and Foundation Engineering, Istanbul, 4, pp. 2527–2606.

Priestley, M.J.N., Seible, F., Calvi, Gl.M., 1996. Seismic Design and Retrofit of Bridges. John Wiley & Sons – Intersciences, New York.

Reese, L.C., Cox, W.R., Koop, F.D., 1975. Field testing and analysis of laterally loaded piles in stiff clay. 7th Annual Offshore Technology Conference, Houston, Texas, 2, pp. 672–690.

Reese, L.C., Van Impe, W.F., 2001. Single Piles and Pile Groups Under Lateral Loading. Balkema, Rotterdam, 463.

Reese, L.C., Welch, R.C., 1975. Lateral loading of deep foundations in stiff clay. J. Geotech. Eng. Div., 101; 633–649.

Remaud, D., Garnier, J., Frank, R., 1998. Laterally loaded piles in dense sand: group effects. In: Proceedings of International Conference on Centrifuge 98, Tokyo, 1, pp. 533–538.

Rollins, K.M., Lane, J.D., Gerber, T.M., 2005. Measured and computed lateral response of a pile group in sand. J. Geotech. Geoenviron. Eng. ASCE 131 (1), 103–114.

Ruesta, P.F., Townsend, F.C., 1997. Evaluation of laterally loaded pile group at Roosevelt Bridge. J. Geotech. Geoenviron. Eng. 123, 1153–1161.

Yang, Z., Jeremic, B., 2002. Numerical analysis of pile behaviour under lateral loads in layered elastic-plastic soils. Int. J. Numer. Anal. Methods Geomech. 26 (14), 1385–1406.